Journal of the Korean Magnetic Resonance Society **2012**, *16,* 172-184

Backbone NMR Assignments of a Prokaryotic Molecular Chaperone, Hsp33 from *Escherichia coli*

Yoo-Sup Lee and Hyung-Sik Won*

Department of Biotechnology, Konkuk University, Chungju, Chungbuk 380-701, Republic of Korea
(Received Nov 6, 2012 ; Revised Nov 30, 2012 ; Accepted Dec 10, 2012)

Abstract : The prokaryotic molecular chaperone Hsp33 achieves its holdase activity upon response to oxidative stress particularly at elevated temperature. Despite many structural studies of Hsp33, which were conducted mainly by X-ray crystallography, the actual structures of the Hsp33 in solution remains controversial. Thus, we have initiated NMR study of the reduced, inactive Hsp33 monomer and backbone NMR assignments were obtained in the present study. Based on a series of triple resonance spectra measured on a triply isotope-[^{2}H/^{13}C/^{15}N]-labeled protein, sequence-specific assignments of the backbone amide signals observed in the 2D-[^{1}H/^{15}N]TROSY spectrum could be completed up to more than 96%. However, even considering the small portion of non-assigned resonances due to the lack of sequential connectivity, we confirmed that the total number of observed signals was quite smaller than that expected from the number of amino acid residues in Hsp33. Thus, it is postulated that peculiar dynamic properties would be involved in the solution structure of the inactive Hsp33 monomer. We expect that the present assignment data would eventually provide the most fundamental and important data for the progressing studies on the 3-dimensional structure and molecular dynamics of Hsp33, which are critical for understanding its activation process.

Keywords: Hsp33, oxidative stress, triple resonance, backbone NMR assignments

INTRODUCTION

The majority of general heat shock proteins function as molecular chaperones under heat-stressed conditions of cells, to prevent degradation of cellular macromolecules.[1] However, the prokaryotic

Department of Biotechnology, Konkuk University, Chungju, Chungbuk 380-701, Republic of Korea
Tel: +82.43.840.3589 Fax: +82.43.852.3616 email: wonhs@kku.ac.kr
Journal of the Korean Magnetic Resonance Society 2012 December; 16(2): 172-184
http://dx.doi.org/10.6564/JKMRS.2012.16.2.172

molecular chaperone Hsp33 is distinctive in that it protects cells from acute oxidative stress.[2,3] The expression of Hsp33 is also up-regulated by heat at transcriptional level, but the post-translational activation of the protein is dependent on the cellular redox potential. Thus, the activated Hsp33 functions to cope with the oxidative heat condition and/or a severe oxidative stress. Under normal, reducing condition, Hsp33 exists as an inactive, monomeric form that binds a zinc ion via four conserved cysteines at the C-terminal redox-switch domain. It is generally known that the activation process of the inactive Hsp33 monomer is triggered by the oxidation of the conserved cysteines leading to the formation of two intra-molecular disulfide bonds with releasing the zinc ion. Releasing zinc results in the unfolding of the C-terminal, redox-switch domain and finally the protein, as forming dimers and/or oligomers, can achieve a holdase activity that binds folding intermediates of substrate proteins to prevent their ultimate, irreversible denaturation.[1-6]

Several crystal structures of Hsp33 are already available for the Hsp33 from different species and many biochemical and structural studies have been successful in revealing the molecular mechanism of chaperone function.[7-11] In particular, recent investigations by Reichmann *et al.* suggested a structural mechanism for the holdase activity of the activated Hsp33 to act on denaturing substrates.[12] Thus, the Hsp33 has been evaluated as an ideal molecule for in-depth structural analysis of chaperone mechanism.[13] Nonetheless, a detailed process of the oxidation-induced activation of Hsp33 still remains controversial at the structural level, due to limitations of known structural information, which has been provided mainly by X-ray crystallography. In particular, Hsp33 can adopt several different conformations according to redox status and functional situation, including the reduced monomer,

oxidized monomer, oxidized dimer, reduced dimer, and oxidized oligomer forms. However, the known crystal structures were not sufficient to elucidate all of the different conformations and contained many doubtful features in physiological relevance.[14,15] All those uncertainties raised the needs of complementary structural study of Hsp33 by NMR in solution. Thus, in the present study, we report the backbone resonance assignments of the reduced, inactive monomeric form of Hsp33, as the first step of NMR-based structural investigation.

EXPERIMENTAL METHODS

The recombinant Hsp33 was prepared from the overproducing *E. coli* strain BL21(DE3)pLysS containing the plasmid pUJ30 that encodes the Hsp33 from *Escherichia coli*.[2] The cells were grown at 37 °C in M9 minimal medium, which was prepared with D_2O and supplemented with [^{15}N]NH_4Cl and [^{13}C]glucose, as the sole source of nitrogen and carbon, respectively, to produce the triply isotope-[^{2}H/^{13}C/^{15}N]-enriched protein. When the A_{600} of cell growth reached about 0.6, protein expression was induced by adding IPTG at a final concentration of 1 mM. Prior to the induction by IPTG, 1mM $ZnSO_4$ was added to produce the protein as a zinc-bound form. After 6 hrs induction, cells were harvested by centrifugation and resuspended in a 25 mM Tris-HCl buffer at pH 7.5. Additionally, 50 μM $ZnSO_4$ and 5 mM dithiothreitol (DTT) was consistently contained in all buffer solutions used, to keep the Hsp33 protein as the inactive monomer form (reduced, zinc-bound form). Cells were disrupted by sonication at 4 °C, and from the supernantant Hsp33 was purified by

sequential applications of various chromatographies: two steps of anion exchange chromatography on a HiTrap Q-Sepharose FF and a HiTrap Q HP column (GE Healthcare), adsorption chromatography on a hydroxyapatite column (Bio-Rad), and gel-permeation chromatography on a HiLoad 16/60 Superdex 75 column (Pharmacia). Finally, the purified solution was concentrated to 0.6 mM for NMR measurements in a 20 mM Tris-HCl buffer (pH 7.4) containing 50 mM NaCl, 5 mM DTT, 20 μM $ZnSO_4$, and 7% D_2O. Monomeric state of the purified Hsp33 was confirmed by the gel-filtration analysis[14-17] and the concentration was estimated spectrophotometrically, using the molar absorptivity (19,285 $M^{-1}cm^{-1}$ at 280 nm) predicted from the amino acid sequence. Conventional 2D-[$^{1}H/^{15}N$]TROSY and a series of TROSY-based triple resonance spectra {HNCA, HN(CO)CA, HNCACB, HN(CO)CACB, HNCO and HN(CA)CO} of the [$^{13}C/^{15}N/^{2}H$]Hsp33 were acquired at 298 K on a Bruker Biospin Avance 900 spectrometer equipped with a cryoprobe. All NMR spectra were processed using NMRPipe/NMRDraw software and analyzed with NMRView program. Chemical shifts were referenced directly to DSS for ^{1}H and indirectly for ^{15}N and ^{13}C atoms using the chemical shift ratios suggested in the BMRB (http://www.bmrb.wisc.edu).

RESULTS AND DISCUSSION

Approximately 12 mg of the purified [$^{13}C/^{15}N/^{2}H$]Hsp33 was finally obtained via 1 L culture and subjected to NMR measurements. The solution structure of the isolated redox-switch domain (residues 227-287) of Hsp33 has been previously solved by NMR spectroscopy.[5] Thus, in the present

study, we employed the same experimental condition for NMR experiments of the intact (residues 1-294) Hsp33: pH 7.4 and 298K. As showing in Fig. 1, the 2D-[^{1}H/^{15}N]TROSY spectrum of the [^{13}C/^{15}N/^{2}H]Hsp33 was obtained with a good dispersion and narrow line widths of amide resonances.

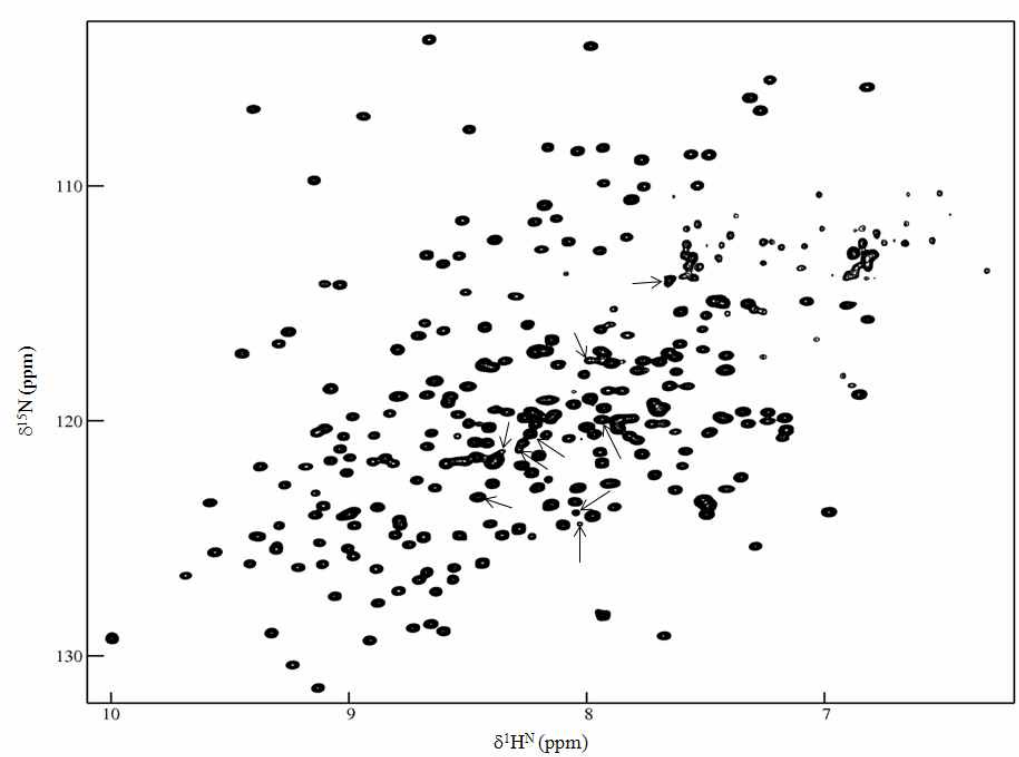

Figure 1. 2D-[^{1}H/^{15}N]TROSY spectrum of the [^{13}C/^{15}N/^{2}H]Hsp33 measured on a 900 MHz NMR machine with a cryoprobe at 298K. The protein was prepared as a reduced, zinc-bound monomer form at pH 7.4. Arrows indicate the resonances that were verified as backbone amide signals, but could not be finally assigned due to lack of sequential connectivity.

For sequence-specific assignments of the backbone amide resonances in the 2D-[^{1}H/^{15}N]TROSY spectrum, we first verified peak clusters of individual resonances by collecting related peaks in the triple resonance spectra.

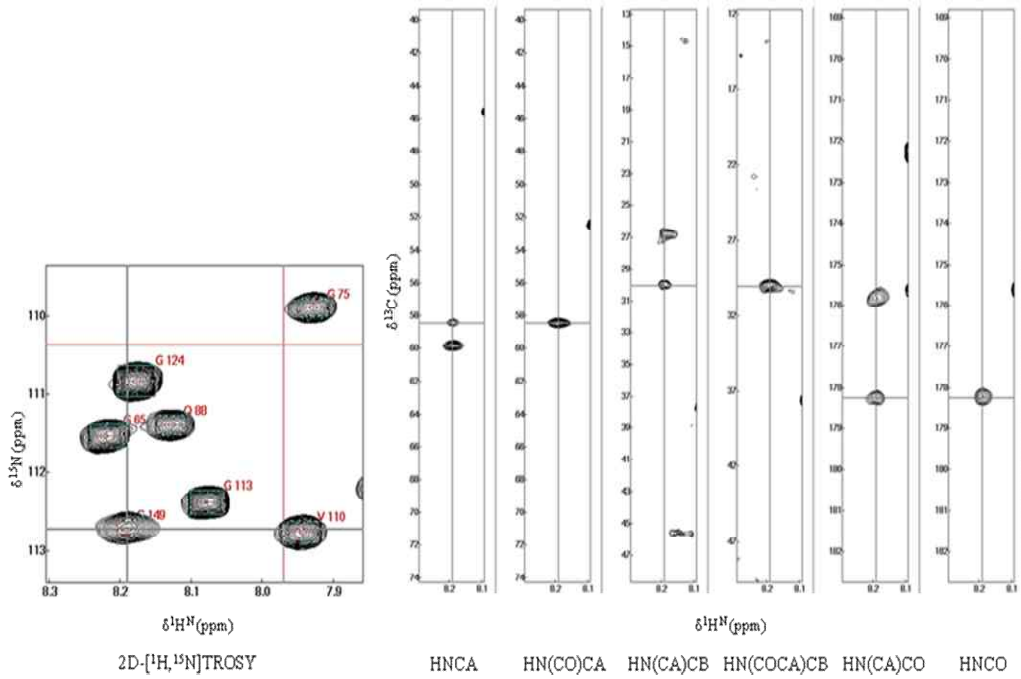

Figure 2. Verification of a peak cluster. A selected region taken from the 2D-[^{1}H/^{15}N]TROSY spectrum (Fig. 1) was enlarged in the left panel and the other strip plots for the triple resonance spectra were taken from the slices with the ^{15}N chemical shift of 112.7 ppm. The x-axis of the individual spectrum represents the ^{1}H chemical shift. The y-axes represent the ^{13}C chemical shifts in the triple resonance spectra, while ^{15}N chemical shifts in the 2D-[^{1}H/^{15}N]TROSY spectrum. The 10 peaks with the same $^{1}H^{N}$ (8.20 ppm) and ^{15}N (112.7 ppm) chemical shift are combined into a peak cluster.

Because all of the backbone NMR signals originating from the same residue manifest the same $^{1}H^{N}$ and ^{15}N chemical shifts in individual spectra, the corresponding peaks could be combined into a

peak cluster. As illustrated for the S149 residue in Fig. 2, a single peak cluster is composed of ideally 10 peaks with the same amide $^{1}H^{N}/^{15}N$ chemical shifts in the 2D-[$^{1}H/^{15}N$]TROSY and six kinds of triple resonance spectra. Thus, each peak cluster additionally contains chemical shift information about the intra- and inter-residue carbon atoms: $^{13}C^{\alpha}$(i) and $^{13}C^{\alpha}$(i-1) from the HNCA and HN(CO)CA spectra, $^{13}C^{\beta}$ (i) and $^{13}C^{\beta}$ (i-1) from the HN(CA)CB and HN(COCA)CB spectra, and ^{13}C'(i) and ^{13}C' (i-1) from the HN(CA)CO and HNCO spectra. The $^{13}C^{\alpha}$, $^{13}C^{\beta}$ and ^{13}C' chemical shift values were also useful for prediction of the spin systems of individual clusters. In this way, totally 255 peaks in the 2D-[$^{1}H/^{15}N$]TROSY spectrum was confirmed as backbone amide resonances with reasonable patterns of peak clusters. All the other signals in the 2D-[$^{1}H/^{15}N$]TROSY spectrum could be also verified unambiguously as side-chain signals from Gln, Asn, Arg, and Trp residues. Then, sequence-specific assignments could be achieved by the sequential linking of the peak clusters, according to the inter-residue ^{13}C connectivities of each cluster. As a representative example, Fig. 3 depicts the sequential, amino-acid specific linking in the region V130 to D136, according to the intra- and inter-residue ^{13}C' correlations observed in the HN(CA)CO spectrum. Likewise, the $^{13}C^{\alpha}$ and $^{13}C^{\beta}$ connectivities were traced in the HNCA and the HN(CA)CB spectrum, respectively (data not shown). The other spectra, HNCO, HN(CO)CA and HN(COCA)CB, were used to confirm the inter-residue ^{13}C', $^{13}C^{\alpha}$ and $^{13}C^{\beta}$ correlations, respectively.

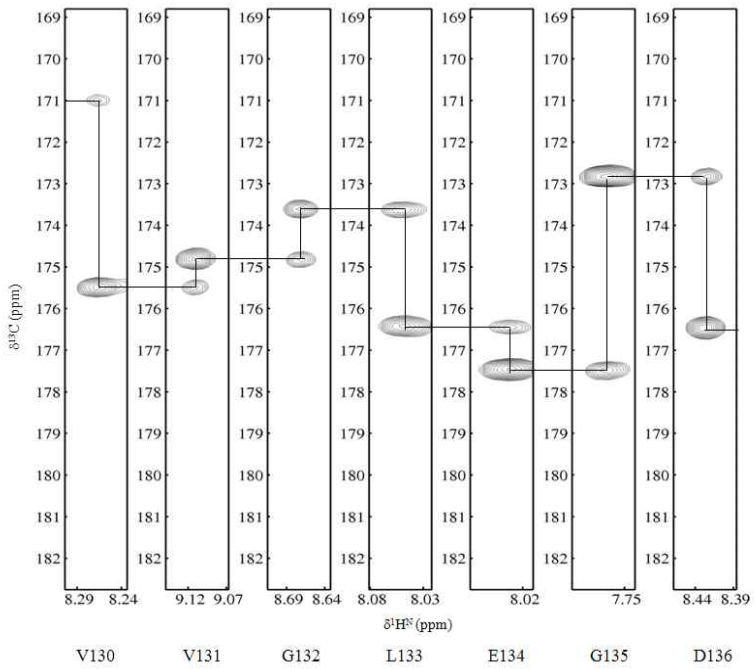

Figure 3. Sequential linking of peak clusters according to the intra- and inter-residue $^{13}C'$ correlations. Selected strips from the 3D TROSY-HN(CA)CO spectrum are presented. Solid lines show the connectivities for the region V130 to D136.

Finally, the sequence specific assignments were obtained for total 246 resonances, which correspond to approximately 96.5% assignments of the observed backbone signals (255 peaks) in the 2D-[$^{1}H/^{15}N$]TROSY spectrum. The finally assigned backbone amide $^{1}H^{N}$ and ^{15}N chemical shifts are summarized in Table 1. Among the 255 peaks in the 2D-[$^{1}H/^{15}N$]TROSY spectrum that were identified as backbone amide resonances, just nine signals could not be assigned (Fig. 1) due to the lack of sequential connectivity, despite clear observation of peak clusters. In addition, the results in Table 1 involve a few ambiguous assignments, such as the M3, Y39, Q41 and L57 residues, which

were determined depending on just ^{13}C chemical shift values without sufficient inter-residue connectivity.

Table 1. $^{1}H^{N}$ and ^{15}N chemical shifts (ppm) assigned in the 2D-[$^{1}H/^{15}N$]TROSY spectrum of the reduced, zinc-bound Hsp33 at 298 K and pH 7.4 (NA, not available; ND not detected).

a.a.	$^{1}H^{N}$	^{15}N	a.a.	$^{1}H^{N}$	^{15}N	a.a.	$^{1}H^{N}$	^{15}N	a.a.	$^{1}H^{N}$	^{15}N
M1	NA	NA	G75	7.94	109.9	S149	8.20	112.7	Y223	8.37	126.4
I2	NA	NA	P76	NA	NA	E150	ND	ND	D224	8.51	120.1
M3	8.45	126.1	M77	8.18	120.6	Q151	7.45	114.8	P225	NA	NA
P4	NA	NA	N78	7.43	117.8	L152	7.21	118.9	Q226	8.66	120.5
Q5	ND	ND	L79	7.33	120.1	P153	NA	NA	D227	8.68	126.4
H6	ND	ND	A80	8.80	127.2	T154	7.80	120.8	V228	7.49	123.5
D7	ND	ND	V81	9.09	121.7	R155	9.40	124.9	E229	8.65	122.9
Q8	7.72	119.5	I82	8.42	124.4	L156	9.60	123.5	F230	8.56	121.7
L9	9.32	125.5	N83	8.80	124.4	F157	8.91	120.6	K231	7.69	129.2
H10	ND	ND	G84	9.16	109.8	I158	9.01	124.0	C232	8.61	129.0
R11	ND	ND	N85	7.33	115.0	R159	9.07	127.5	T233	8.31	114.7
Y12	ND	ND	N86	8.55	113.0	T160	8.40	112.3	C234	7.89	123.7
L13	9.01	121.6	N87	7.80	117.9	G161	8.05	108.5	S235	7.50	108.7
F14	8.62	123.3	Q88	8.14	111.4	D162	8.24	122.2	R236	9.15	124.0
E15	ND	ND	Q89	6.83	115.7	V163	8.86	121.6	E237	8.65	118.3
N16	9.11	114.2	M90	8.91	121.7	D164	9.34	129.0	R218	7.88	120.4
F17	7.09	114.9	R91	8.62	113.3	G165	8.68	103.8	C239	7.70	119.6
A18	ND	ND	G92	8.00	104.1	K166	7.73	122.3	A240	8.47	123.2
V19	ND	ND	V93	8.81	119.0	P167	NA	NA	D241	7.67	117.1
R20	9.32	125.4	A94	7.51	124.0	A168	8.22	122.8	A242	7.36	122.4
G21	8.51	107.6	R95	9.03	120.7	A169	8.17	119.1	L243	7.98	120.6
E22	8.43	116.9	V96	8.23	120.1	G170	8.95	107.0	K244	7.64	117.3
L23	9.04	124.1	Q97	9.39	124.9	G171	9.42	106.8	T245	7.28	106.8
V24	9.70	126.6	G98	7.82	110.6	M172	9.31	116.7	L246	6.99	123.9
T25	7.84	116.4	E99	8.24	119.6	L173	8.99	123.9	P247	NA	NA
V26	8.42	110.7	I100	8.55	124.9	L174	9.14	125.2	D248	8.70	125.0
S27	ND	ND	P101	NA	NA	Q175	9.28	122.7	E249	9.27	116.2
E28	ND	ND	E102	8.48	120.9	Q176	7.30	125.4	E250	7.18	119.9
T29	ND	ND	N103	8.72	116.4	Q177	7.90	122.7	V251	7.35	119.6
L30	ND	ND	A104	7.17	120.4	Q178	NA	NA	D252	8.58	119.0
Q31	8.35	117.4	D105	7.78	121.4	Q179	8.5	121.5	S253	7.62	115.4
Q32	7.52	117.0	L106	8.22	119.8	Q180	7.94	117.4	I254	7.64	123.0
I33	7.64	120.5	K107	8.26	115.9	Q181	8.44	117.6	L255	8.15	119.8
L34	7.30	117.1	T108	8.02	118.0	Q182	8.16	123.6	A256	7.96	121.4
E35	7.44	119.9	L109	7.95	120.0	Q183	9.19	122.0	E257	7.62	116.7
N36	8.69	115.8	V110	7.96	112.8	Q184	8.90	126.3	D258	8.41	117.7
H37	7.48	114.9	G111	7.77	110.0	Q185	8.81	117.0	G259	8.18	108.4
D38	ND	ND	N112	9.02	125.4	Q186	7.25	120.0	E260	7.44	115.0
Y39	8.01	120.3	G113	8.09	112.4	Q187	7.60	121.3	I261	9.05	121.2

P40	NA	NA	Y114	8.61	116.2	Q188	8.79	118.9	D262	8.74	128.8
Q41	8.14	119.6	V115	9.00	119.8	Q189	7.83	120.6	M263	8.99	125.8
P42	NA	NA	V116	9.22	126.2	Q190	7.59	118.5	H264	8.60	121.8
V43	6.92	115.1	I117	9.14	131.4	Q191	8.72	126.8	C265	8.65	127.3
K44	7.69	119.5	T118	9.12	123.6	Q192	8.19	117.1	D266	8.93	129.4
N45	7.95	116.1	I119	9.25	130.4	Q193	7.42	119.9	Y267	9.15	120.5
V46	7.25	119.6	T120	8.99	124.5	Q194	7.53	116.1	C268	8.45	117.5
L47	8.09	120.8	P121	NA	NA	Q195	7.43	117.8	G269	7.84	112.2
A48	7.82	119.9	S122	9.09	118.6	Q196	6.83	105.8	N270	8.73	122.5
E49	7.95	117.0	E123	7.94	119.5	I197	7.50	123.6	H271	8.16	116.6
L50	8.84	119.7	G124	8.19	110.8	K198	8.67	128.7	Y272	9.02	122.2
L51	8.76	125.3	E125	8.27	119.9	T199	9.15	123.1	L273	8.37	124.9
V52	7.92	118.7	R126	8.41	122.7	E200	9.46	117.1	F274	9.31	124.5
A53	8.68	118.9	Y127	8.80	124.2	E201	6.86	118.9	N275	9.39	121.9
T54	8.52	114.5	Q128	8.11	124.4	L202	7.43	117.2	A276	8.60	119.2
S55	8.28	121.0	G129	9.05	114.2	L203	7.57	108.7	M277	8.07	119.3
L56	ND	ND	V130	8.28	121.9	T204	7.24	105.5	D278	8.41	121.9
L57	8.82	121.8	V131	9.12	126.1	L205	7.52	123.4	I279	8.35	119.6
T58	ND	ND	G132	8.68	113.0	P206	NA	NA	A280	7.91	122.7
A59	6.90	118.5	L133	8.06	123.5	A207	8.57	126.3	E281	7.70	117.5
T60	7.55	110.0	E134	8.05	122.9	N208	8.54	111.5	I282	7.86	119.9
L61	7.42	122.9	G135	7.78	108.9	E209	7.19	120.7	R283	8.13	117.6
K62	8.39	121.6	D136	8.44	116.0	V210	7.61	121.9	N284	7.91	117.6
F63	7.50	120.5	T137	7.33	106.3	L211	7.92	115.9	N285	8.00	119.1
D64	8.43	120.9	L138	9.58	125.6	W212	7.69	120.1	A286	7.99	124.1
G65	8.23	111.5	A139	9.11	120.3	R213	8.07	118.8	S287	8.23	117.1
D66	7.73	119.3	A140	7.67	118.5	L214	7.51	115.5	P288	NA	NA
I67	8.55	119.7	C141	7.78	117.4	Y215	ND	ND	A289	8.30	124.6
T68	8.89	123.7	L142	8.16	119.9	H216	ND	ND	D291	8.21	121.5
V69	8.89	127.8	E143	8.68	121.1	E217	ND	ND	P291	NA	NA
Q70	8.82	124.9	D144	7.74	120.1	E218	ND	ND	Q292	8.42	120.3
L71	9.43	126.1	Y145	7.88	120.1	E219	ND	ND	V293	7.95	121.8
Q72	8.53	121.7	F146	8.40	119.5	V220	ND	ND	H294	7.94	128.3
G73	7.94	108.4	M147	7.86	118.7	T221	8.81	125.6			
D74	7.64	117.9	R148	8.51	118.5	V222	8.57	126.8			

As Hsp33 is 294 amino acids long, including 14 prolines, total 279 (294 residues minus 14 prolines and the N-terminal residue) backbone amide resonances are expected to be detected in the NMR spectra. Thus, the present results (246 residues assignments) correspond to about 88% complement of possible amide resonance assignments. However, even including the non-assigned peaks in the 2D-[^{1}H/^{15}N]TROSY spectrum, the number of backbone amide resonances observed (255 peaks) are just 91% of the ideal detection. In other words, it can be estimated that the resonance

signals from at least about 8 ~ 13 % (25 ~ 39 amino acids) residues were not detected in the NMR spectra. We used a highly deuterated protein to overcome the short relaxation time (T_2) due to long molecular tumbling time, which is expected from the high molecular weight (33 kDa) of Hsp33. Judged from the overall quality (good dispersion and narrow linewidth) of the spectra, which were measured using a ultra-highfield (900 MHz) NMR machine with a cryoprobe, the significant portion of missing signals are not attributable to the high molecular weight of Hsp33. In addition, based on the known crystal structures, the non-assigned regions are not varied in the core of the protein, which rule out the possibility of non-exchangeable amide deuterium of the protein sample. Then, in general, some residues of a protein, particularly at loop regions, may not show up their NMR peaks due to a certain dynamic fluctuation at an intermediate time scale, which results in severe line broadening. However, the non-assigned or non-detected regions contain well-structured elements based on known crystal structures of Hsp33 and are mapped mainly onto the N-terminal regions. Thus, we hypothesize that the non-detected signals would represent a peculiar dynamic motion existing in the reduced, inactive Hsp33 monomer in solution, which is not observed in the crystal structures. To check the possibility, it is required to perform NMR analysis under various experimental conditions with different pH, temperature and magnetic field. In addition, there is no doubt that NMR will be the most appropriate tool to characterize the molecular dynamics of Hsp33 and the present assignment results will provide fundamental information for that analysis. Then, biological significance of the dynamic properties, whether those are critically associated with the chaperone activity and/or functional regulation of Hsp33, is worthy of further investigation. Finally, the present results suggest

that the Hsp33 structure in solution would include different properties from those observed in the known crystal structures. Thus, we expect that the present result will significantly contribute to progressing investigation of the solution structure of Hsp33.

Acknowledgments

This work was supported mainly by Basic Science Research Program (no. 2010-0006022) through the National Research Foundation of Korea (NRF) funded by the Ministry of Education, Science and Technology, and in part by the Korea Healthcare Technology R&D project, Ministry for Health, Welfare & Family Affairs, Republic of Korea [A092006]. This study made use of the NMR facility at the Korea Basic Science Institute, which is supported by the KBSI high-field NMR research program.

REFERENCES

1. L. Tutar, Y. Tutar, *Curr. Pharm. Biotechnol*. **11**, 216 (2010).
2. U. Jakob, W. Muse, M. Eser, J.C.A. Bardwell, *Cell* **96**, 341 (1999).
3. J. Winter, M. Ilbert, P.C. Graf, D. Ozcelik, U. Jakob, *Cell* **135**, 691 (2008).
4. M. Ilbert, J. Horst, S. Ahrens, J. Winter, P.C.F. Graf, H. Lilie, U. Jakob, *Nat. Struct. Mol. Biol.* **14**, 556 (2007).
5. H.-S. Won, L.Y. Low, R.D. Guzman, M. Martinez-Yamout, U. Jakob, H.J. Dyson, *J. Mol. Biol.* **341**, 893 (2004).
6. C.M. Cremers, D. Reichmann, J. Hausmann, M. Ilbert, U. Jakob, *J. Biol. Chem*. **285**, 11243 (2010).

7. I. Janda, Y. Devedjiev, U. Derewenda, Z. Dauter, J. Bielnicki, D.R. Cooper, P.C.F. Graf, A. Joachimiak, U. Jakob, Z.S. Derewenda, *Structure* **12**, 1901 (2004).
8. J. Vijayalakshmi, M.K. Mukhergee, J. Graumann, U. Jakob, M.A. Saper, *Structure* **9**, 367 (2001).
9. S.-J. Kim, D.-G. Jeong, S.-W. Chi, J.-S. Lee, S.-E. Ryu, *Nat. Struct. Biol.* **8**, 459 (2001).
10. L. Jaroszewski, R. Schwarzenbacher, D. McMullan, P. Abdubek, S. Agarwalla, E. Ambing, H. Axelrod, T. Biorac, J.M. Canaves, H.-J. Chiu, *et al*., *Proteins* **61**, 669 (2005).
11. S-W. Chi, D.G. Jeong, J.R. Woo, H.S. Lee, B.C. Park, B.Y. Kim, R.L. Erikson, S.E. Ryu, S.J. Kim, *FEBS Lett.* **585**, 664 (2011).
12. D. Reichmann, Y. Xu, C.M. Cremers, M. Ilbert, R. Mittelman, M.C. Fitzgerald, U. Jakob, *Cell* **148**, 947 (2012).
13. M.P. Mayer, *Cell* **148**, 843 (2012).
14. Y.-S. Lee. K.-S. Ryu, S.-J. Kim, H.-S. Ko, D.-W. Sim, Y.-H. Jeon, E.-H. Kim, H.-S. Won, *FEBS Lett.* **586**, 411 (2012).
15. Y.-S. Lee, K.-S. Ryu, Y. Lee, S. Kim, K.W. Lee, H.-S. Won, *J. Kor. Magn. Reson. Soc.* **15**, 137 (2011).
16. Y.-S. Lee, H.-S. Ko, K.-S. Ryu, Y.-H. Jeon, H.-S. Won, *J. Kor. Magn. Reson. Soc.* **14**, 117 (2010).
17. D.-W. Sim, Y.-S. Lee, J.-H. Kim, M.-D. Seo, B.-J. Lee, H.-S. Won, *BMB Rep*. **42**, 387 (2009).